EFFECTS OF THE THERMAL CHARACTERISTICS OF SNOW ENTRAINMENT IN AVALANCHE RUN-OUT AT BIRD HILL, SOUTH-CENTRAL ALASKA

Katreen Wikstroem Jones[1]*, David Hamre[2] and Perry Bartelt[3]

[1]Alaska Pacific University, Anchorage, AK, USA
[2]Alaska Railroad Corporation, Anchorage, AK, USA
[3]WSL Institute for Snow and Avalanche Research SLF, Davos, Switzerland

ABSTRACT: Snow entrainment has a large impact on avalanche flow regime. It adds mass to the moving avalanche body which can amplify a fluidized or lubricated flow regime. Recent studies have demonstrated the importance of the thermal characteristics of the entrained snow for avalanche rheology. Fluidization and lubrication, typical for dry respectively wet avalanches, lead to increased run-out distance, velocity and impact pressure. At Bird Hill, located south-east of Anchorage, Alaska, along the Seward Highway and the Alaska Railroad, small avalanches have historically produced unexpectedly large and fast avalanches with long run-out distances. Deposition of large debris piles on the highway and the railroad indicate significant snow entrainment. Bird Hill is unique for its maritime sub-arctic snowpack, small release zones, consistent steep slopes and minimal transition zones. In this project we will implement the 2-D dynamical run-out model RAMMS in order to examine the impact that the thermal snow cover properties in the avalanche path have on avalanche flow regimes after entrainment. In agreement with current research, our early simulation results, presented in this paper, show that for avalanches to starve at the steep slopes of Bird Hill, snow cover temperature and density is equally or even more critical than the amount of entrained mass along the avalanche track. Snow cover characteristics can be correlated to weather data and monitored from weather station data. Our final project results may explain particular avalanche behaviors at Bird Hill that can improve run-out assessments and thereby support decision-making of road closures at this dangerous highway and railroad corridor.

KEYWORDS: snow entrainment, snow temperature, avalanche run-out, flow regimes, fluidization, lubrication

1. INTRODUCTION

The flow regime defines the avalanche flow behavior and deposit characteristics (Gauer et al, 2008). Avalanches have two general flow regimes: dry and wet (moist). Both regimes produce far reaching flows that exert significant impact pressures on obstacles. Snow temperature is important as it defines the rheology of the flowing snow. Granularization of dry snow produces fast moving dispersed/fluidized flows with a significant powder part while wet (moist) snow produces dense flows with pronounced viscous properties. Snow entrainment influences the flow regime because it supplies the avalanche with mass at a certain temperature. Entrainment of cold snow feeds the fluidization regime of a dry avalanche, whereas entrainment of warm (close to 0° C) snow

adds thermal heat to the avalanche which accelerates meltwater production. A lubrication effect from meltwater would explain the far-reaching, but slow-moving velocities of wet snow avalanches.

Vera Valero et al (2012) stressed the importance of monitoring snowpack temperatures since they found that the temperature of the entrained snow is capable of completely determining the temperature regime of the avalanche. Based on measurements of snow temperature in their sample of avalanche events, Steinkogler et al (2014) found that after entrainment of snow warmer than -2°C the avalanches showed distinct behavioral change; front velocities and powder clouds decreased rapidly and the resulting debris had levee and finger shapes, typical for warm avalanches.

Amplified fluidization and lubrication flow regimes can increase the run-out distance of relatively small avalanche release volumes which is of concern for railroad and highway avalanche safety operations. The problem of avalanche flow regime and snow cover entrainment/temperature is particularly apparent in the Chugach Mountains, south-central Alaska. Bird Hill, south-east of Anchorage,

* Corresponding author address:
Katreen Wikstrom Jones, Alaska Pacific University, Anchorage, AK, USA 99508;
tel: +1907-268-8051;
email: kwikstroem@alaskapacific.edu

is one of the most problematic avalanche forecasting zones for the Alaska Department of Transportation & Public Facilities and the Alaska Railroad Corporation. At Bird Hill small avalanches (< 25 000 m^3 release volume) have historically produced unexpectedly large and fast avalanches, exhibiting surprisingly long run-out distances and deposition of large debris piles on the highway and the railroad.

Fig. 1: Minimal transition zone at Bird Hill; the 1979 avalanche cycle generated avalanches of design magnitude (AKDOT&PF, 2014).

In this paper we apply a numerical avalanche dynamics model to simulate avalanche scenarios in one of the avalanche paths, #934 Whiskey, at Bird Hill. Our goal is to investigate how track conditions affect the run-out of small avalanches that are difficult to predict (M. Murphy (personal communication)). The hypothetical, yet realistic avalanches that we model represent various combined release masses and erosion depths of varying released snow and entrained snow cover temperatures. We first present an overview of the mechanics of flow regimes. Then we discuss the Bird Hill site, the avalanche run-out model and simulation results.

We show that snow cover temperature, modification of flow regime and the influence of avalanche terrain are all elements of the entrainment problem. The significantly long run-out distances in #934 Whiskey of the small release volumes we simulate are results of snow entrainment on low frictional terrain. Lack of meltwater production in colder (< -1°C entrained snow) avalanches appears to be the stopping factor in shorter run-outs. However, after entrainment of snow that is close to 0°C the run-out distance dramatically increases due to meltwater production. It is therefore important to monitor the snow cover conditions at Bird Hill for accurate run-out assessments.

2. AVALANCHE FLOW REGIMES

Fluidization may mechanically operate throughout the entire moving snow column, whereas the mechanics of the lubricated flow regime are concentrated at the base of the avalanche (Erismann and Abele, 2001). Fluidization implies shear deformations over the entire avalanche flow height. Plug flow regimes, which concentrate the shear deformation at the avalanche's running surface are therefore common for wet snow flows (Dent et al, 1998). A change in flow regime can only happen due to change in the underlying terrain, change in shear properties which affect friction or a change in material properties (Bartelt et al, 2007). Without snow influx by entrainment, the shear gradients that develop in the tail will cause the flow height to decrease which directly reduces the basal slip velocity and the tail starts to decelerate consuming snow from the bulk. This explains why avalanches can suddenly starve at steep slopes if they are not fed by intake of additional material at the front (Bartelt et al, 2007).

2.2 *Fluidization regime*

A granular material can act as a fluid without any liquid water present in its composition. The fluidization regime develops when a granular mass (snow avalanche) sets in motion. Internal pressure builds up from particle-particle collisions and collisions between granules and the bed surface (Pudasaini and Hutter, 2007). A dispersive pressure at the bed surface is created which causes dilation or expansion of the avalanche core (Buser and Bartelt, 2011; Buser and Bartelt, 2014). The expansion (i.e. fluidization) of the avalanche cannot be sustained without continual input of mechanical energy (Fig. 2). Without this energy, the flow core collapses to a dense, frictional flow. The mechanical energy to fluidize the core is related to kinetic and potential energy associated with the slope-perpendicular random movements of the snow granules (Bartelt et al., 2006). This energy is produced by shearing processes but dissipates by plastic particle collisions (Bartelt et al, 2012). An important factor driving the fluidization is the frictional properties of the running bed surface. Typical characteristics of the fluidized regime are rapidly increased avalanche core heights, suspension cloud and reduced internal viscosity (Buser and Bartelt, 2014). The increased space between the particles caused by the increased pressure reduces the internal friction of the avalanche core, leading to a prolonged run-out (Pudasaini and Hutter, 2007).
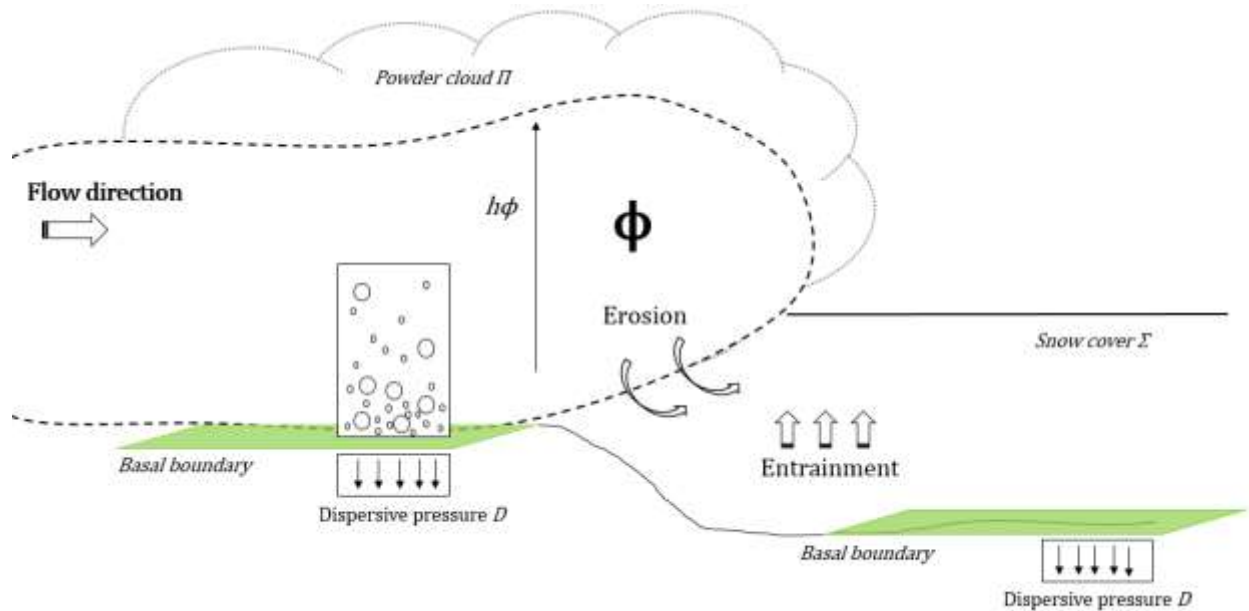
Fig. 2: Dynamics during establishment of basal boundary and dispersive pressure feeding dilation and development into a fluidized regime with an increased core height h_ϕ; momentary relief of dispersive pressure D during entrainment of snow cover Σ and re-establishment of basal boundary.

Snow entrainment momentarily relieves the dispersive pressure by lowering the basal boundary, which decelerate the random particle movements (Fig 2.). However, as a new basal boundary establishes the dispersive pressure re-builds and the kinetic energy associated with the particle fluctuations of the increased snow mass leads to a delayed, but amplified fluidized regime. The effect of snow entrainment on fluidization can be seen on slopes with significant snowpack and/or topographic variations. Snow temperature and density are also critical factors for fluidization. The snow that is being entrained by the avalanche must be cold and dry enough to balance the dissipative thermal energy that is continuously produced from the shear work and random particle collisions. Warm and dense snow limits the fluidization process as more energy is dissipated during the volume expansion (Vera and Bartelt, 2013).

2.3 Lubrication regime

A wet flow regime may develop when liquid water is present within the avalanche body. The presence of meltwater at the basal running surface leads to enhanced gliding. Fluctuations are damped leading to laminar flows with few intergranular interactions and a friction-less surface that the avalanche mass can slide on. When the liquid water content increases within the ice lattice,

the mechanical bonding (shear strength) between the snow grains is reduced (Onesti, 1987). Wet snow clods deform and are molded into rounded shapes hindering the production of slope-perpendicular movements. Liquid water at the bottom of the avalanche therefore rapidly decreases the shear strength and lubricates the avalanche body at its base (Colbeck, 1975). Liquid water may originate from heat dissipated from particle interactions, from kinetically released energy in shear work and from entrainment of warm (close to 0°) snow. Valero et al (2012) found that dissipation of fluctuation energy from random granular interactions are increased with higher snow temperatures. In addition, higher snow temperatures lead to lubrication at the bed surface which reduces friction and therefore shear work (Valero et al, 2012). The concentration of wet granules at the base of the avalanche increases rapidly as a moist snow cover is entrained and because wet granules are less intermixed than dry granules. Therefore, entrainment of warm snow enhances the development of a lubricated flow regime.

3. BIRD HILL, SOUTH-CENTRAL ALASKA

Bird Hill is a south-south east facing ridge with an average elevation of 1000 m, located between Girdwood and Bird Point along the Turnagain Arm south-east of Anchorage in south-central Alaska.

The steepest sections of the slopes (up to 55º) are in the upper elevations above 700 m a s l which translates into on average 30° consistent slopes continuing down to sea level (Fig. 3). The Seward Highway and the Alaska Railroad are situated on a narrow strip of land between the terminus of the slopes and the ocean, cutting through the run-out zones of the avalanche paths. There are no transition zones (~ 10° slope angle) between avalanche track and run-out zone at Bird Hill. Avalanches frequently hit the highway and the railroad. Patches of spruce and alders cover lower elevations between the approximately 25 avalanche paths. Given the uniform topography of the slopes, it is common during an avalanche cycle for several avalanches to release during a short time period. This greatly increases the risk of a catastrophic event where the first avalanche closes the highway traffic allowing multiple cars to collect in adjacent avalanche run-out zones.
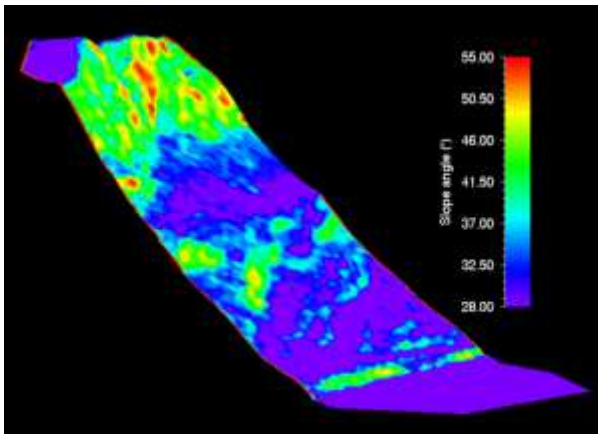

Fig. 3: Slope angles in #934 Whiskey, Bird Hill

4. NUMERICAL SIMULATIONS

In this project, the 2-D dynamical avalanche run-out model RAMMS (Christen et al., 2010) is implemented using a 5 m digital elevation model of Bird Hill and model parameters that represent various snow cover conditions typical for the site. Under an experimental design avalanches are simulated in the avalanche path at Bird Hill named #934 Whiskey (Fig. 3). In RAMMS we analyze the run-out distances, velocities, flow and deposition heights and meltwater production. Run-out distance definitions are based on AKDOT&PF's method; we define the pipeline road as the 80% mark, Old Seward Highway as 100% and the New Seward Highway as 120%.

4.1 RAMMS parameters

In Voellmy's basal shear stress model, the parameter Mu μ is the coefficient for the dry-Coulomb sliding friction and Xi ξ is the coefficient for the turbulent collisional friction in the avalanche core, both projected on the basal sliding surface (Bartelt et al, 2007). In the extended RAMMS model, the Voellmy shear stress $\vec{S}_\phi = (S_{x\phi} S_{y\phi})$ is modified to account for dry and wet avalanche flow regimes:

$$\vec{S}_\phi = \frac{\vec{u}_\phi}{\|\vec{u}_\phi\|} \left[\mu(R,T)[N] + \rho g \frac{\|\vec{u}_\phi\|^2}{\xi(R,T)} \right] \qquad (1)$$

where $\vec{u}_\phi$ is avalanche velocity, R is fluctuation energy, T the avalanche temperature. The total normal pressure N consists of pressures arising from the self-weight, centrifugal accelerations and dispersive pressure (Buser and Bartelt, 2014).

The following functional dependencies for μ and ξ are employed:

$$\mu(R,T) = \mu_0(T) \exp\left[-\frac{R}{R_0} \right] \qquad (2)$$

and

$$\xi(R,T) = \xi_0(T) \exp\left[\frac{R}{R_0} \right]. \qquad (3)$$

Fluidized flow regimes are associated with higher random fluctuation energies. When $R = 0$, the avalanche is a dense frictional regime governed by the non-fluidized friction parameters μ_0 and ξ_0.

The parameter R_0 defines the energy required to activate fluidization and therefore the decrease of the friction as the fluidization process progresses.

To enable analysis of various run-out distances and to produce realistic avalanches at Bird Hill we set $\mu_0 = 0.55$ and $\xi_0 = 1200$ m/s², recommended for channeled terrain below 1000 m a s l. The activation energy is set to $R_0 = 4000$ J/m³. These values are similar to values derived from back calculations of large, dry Vallée de la Sionne avalanches (Bartelt et al, 2012). The avalanche paths at Bird Hill are steep, with minimal transition zones and few terrain features. In addition, we aim to simulate avalanches that release frequently (< 10 year return period).

For detailed description of the governing balance and momentum equations that are numerically solved in RAMMS, see Valero et al (2012) and Bartelt et al (2012). These papers describe the two-parameter method to calculate the fluctuation energy R. One parameter α defines the generation R from the mean flow. This parameter essentially defines the turbulent Reynolds stresses in the flow as it quantifies the energy extracted from the mean flow to create the fluctuations and fluidize the avalanche core. The second parameter β governs the dissipation of random kinetic energy to heat. Thermal heat is considered internal energy E.

Internal energy increases by two processes: (1) the dissipation of mechanical energy and (2) the entrainment of snow. Snow entrainment $\dot{Q}_{\Sigma\to\phi}$ (kg m^{-2}) is given by the relation (Christen et al., 2010; Bartelt et al., 2012):

$$\dot{Q}_{\Sigma\to\phi} = \rho_\Sigma \kappa \|\vec{u}_\phi\|$$

parameterized using the erodibility parameter κ entrainment and the slope parallel velocity $\vec{u}_\phi$. The heat energy associated with $\dot{Q}_{\Sigma\to\phi}$ is considered in the model formulation. The rise in heat energy is therefore a function of the snow density, the amount of in taken snow (parameter κ) and the speed of the avalanche.

4.2 *First results*

We varied the entrainment parameters: erosion depth (ED), entrained snow temperature (TE) and entrained snow density (ρ) in 16 avalanche simulations in RAMMS of identical release conditions: small release volume of 6808 m^3, released snow temperature -5°C and released snow density 200 kg/m^3 (Tbl. 1).

All the avalanches accelerated in the upper steep, channeled section of the path and decelerated around 600 m a s l where the slope lessens to ≈ 30° (Fig. 3). All the ED 0.1 m avalanches stopped at this critical section. The larger avalanches continued flowing beyond this point, exhibiting distinctive flow behavior depending on the temperature and density of the entrained snow cover.

Alternation of entrained mass (ED 0.25 m, 0.35 m and 0.5 m) with the same snow cover temperature did not have a significant impact on run-out distance (Fig. 4). However, velocities and impact pressures varied with these different ED values; max velocities differ in the range of a couple of

m/s and max impact pressures differ by roughly 20 kPa between the simulations (Fig. 6-7).

Tbl. 1: Entrainment parameters;: erosion depth (ED), entrained snow temperature (TE) and entrained snow density (ρ) used for avalanche simulations in #934 Whiskey of release volume 6809 m^3, released snow temperature -5°C and released snow density 200 kg/m^3.

ED (m)	TE (°C)	P (kg/m^3)
0.5	-5	300
0.5	-2	400
0.5	-1	450
0.5	0	500
0.35	-5	300
0.35	-2	400
0.35	-1	450
0.35	0	500
0.25	-5	300
0.25	-2	400
0.25	-1	450
0.25	0	500
0.1	-5	300
0.1	-2	400
0.1	-1	450
0.1	0	500

Of the ED 0.25 m avalanches, TE -5°C had most velocity fluctuations throughout the flow and almost stopped at 400 m a s l where it also reached its peak in flow height. Despite similar run-out distances of ED 0.25 m TE -5°C and ED 0.25 m TE -2°C, three degrees warmer and 100kg/m3 denser entrained snow resulted in a higher max flow height in the upper narrow gully and less significant deposition at ~ 500 m a s l. In the ED 0.25 m TE -1°C avalanche compared to the previous colder flows the most significant result were higher velocities at the end portion of the flow and a more rapid deceleration (Fig. 8). TE 0°C maintained a higher speed through the flatter section at 600 - 400 m a s l and accelerated at the end section of the track after meltwater production initiated (Fig. 9). It also had the lowest average flow heights throughout the flow until large deposition on the road.
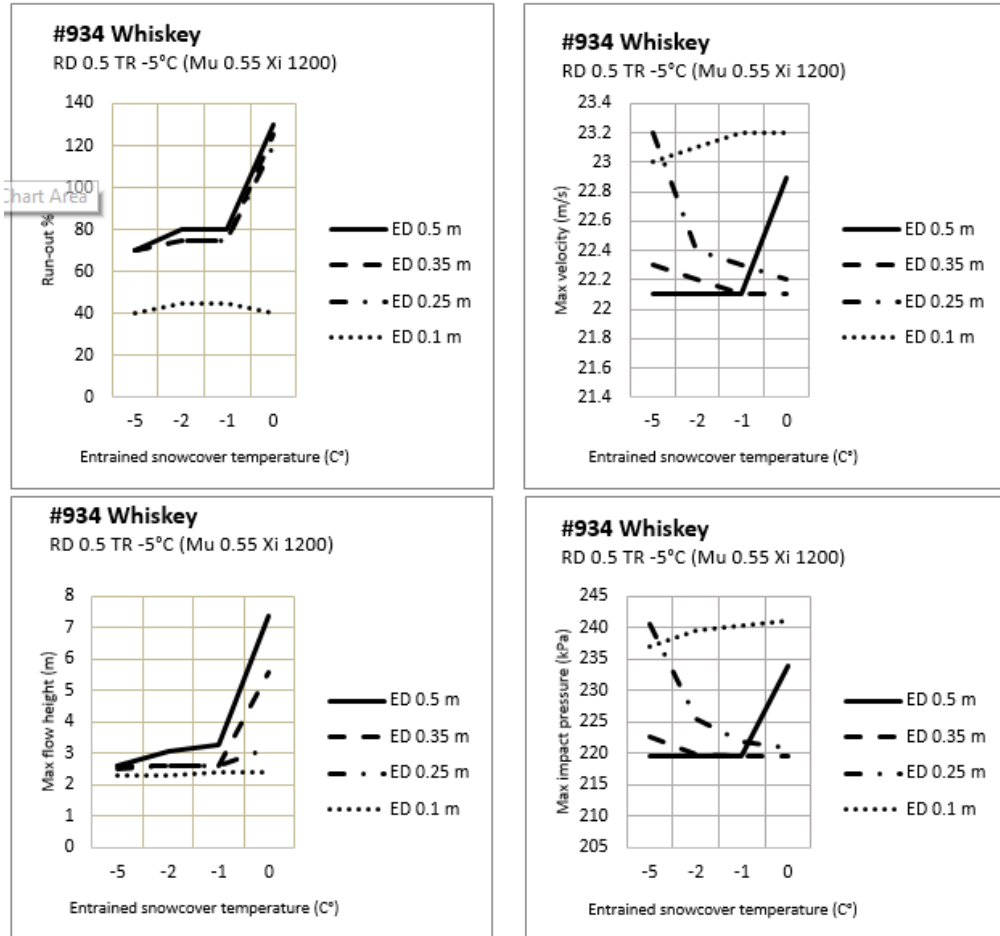
Fig. 4: (Upper left) Run-out distance (% relative to Old Seward highway which is = 100 %. New highway = 120%) for scenario simulations in #934 Whiskey, Bird Hill. Fig. 5: (Lower left) Maximum flow height (m) for scenario simulation in #934 Whiskey, Bird Hill. Fig. 6: (Upper right) Max velocity (m/s) for scenario simulations in #934 Whiskey, Bird Hill. Fig. 7: (Lower right) Max impact pressure (kPa) for scenario simulations in #934 Whiskey, Bird Hill.

Of the ED 0.5 avalanches, TE -5°C, -2°C and -1°C exhibited very similar speed patterns (Fig. 6) of deceleration at 600 m a s l with a small portion that continued and finally starved at ~ 70-80% (Fig. 4). TE 0°C accelerated below 400 m a s l and reached its maximum speed right before deposition on the New Seward Highway; 120% (Fig. 6).

ED 0.5 m TE -5°C reached its highest flow height at ~ 800 m a s l right after exit of the upper gully whereas TE -1°C reached its highest flow height at ~500 m a s l. Like the results for ED 0.25 m, the ED 0.5 m TE 0°C avalanche had on average the lowest flow heights ~ 1 m but deposited up to 6 m of debris on the road.

Due to a larger mass entrained, the ED 0.5 m TE -5°C avalanche deposited more mass in the run-out zone than the ED 0.25 m TE -5°C avalanche,

but it did not reach any longer run-out distance. In addition, the smaller flow of ED 0.25 m generated slightly higher max velocity and max impact pressure.

For all the EDs > 0.25 m, a TE change from -5°C to 0°C resulted in a much longer run-out distance (Fig. 11-12). Meltwater production below 500 m a s l appears to be the cause of the dramatically increased run-out distance (Fig. 10). As we increase the ED from 0.25 m to 0.5 m for two snow cover of the same TE (-5°C) we did not obtain any longer run-out, but the average avalanche temperature decreased significantly (Fig. 12-13).

Despite their short distance of travel, all the ED 0.1 m avalanches had comparably high max velocities and max impact pressures (Fig. 7) with max flow heights not exceeding 2.4 m (Fig. 5). In
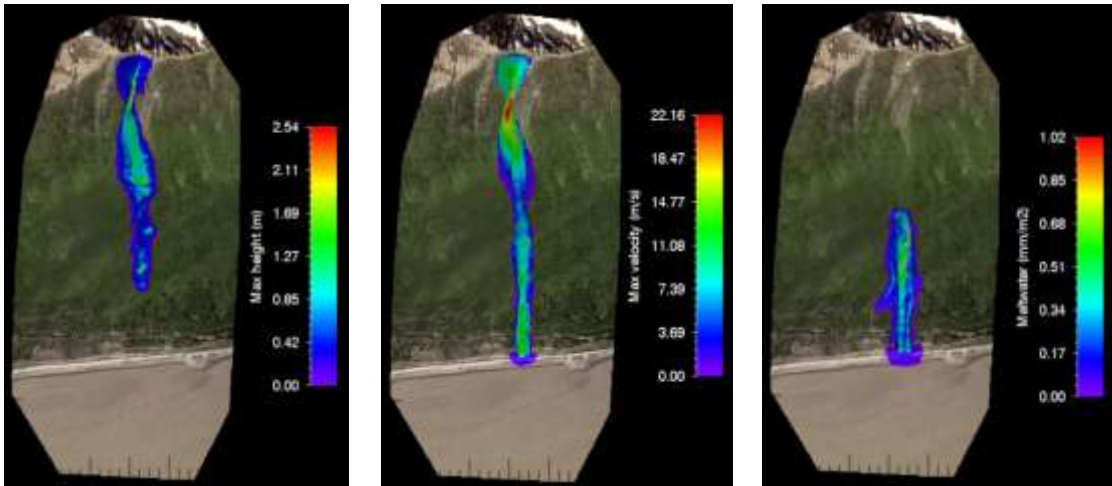
743

Fig. 8: (Left) Max flow heights for ED 0.25 m TE -1°C. Fig. 9: (Middle) Max velocities for ED 0.25 m TE 0°C. Fig. 10: (Right) Meltwater production for ED 0.5 m TE 0°C.

the case of ED 0.1 m we retrieved higher velocities and higher impact pressures with an increasing entrained snow temperature. That relationship is reversed to what we found for the ED 0.25 m and ED 0.35 m simulations. However, for ED 0.5 m, velocity and impact pressure dramatically increased when a 0°C snow cover was entrained (Fig. 6-7).

5. CONCLUSIONS AND FUTURE WORK

Because of the low frictional terrain and steep slope angle of Bird Hill, less heat is produced internally in an avalanche compared to other sites with more rough terrain. Entrainment of a warm (close to °C) snow cover is required for meltwater production to initiate in #934 Whiskey. Tracks with rougher terrain would generate more frictional shear work and thus more heat, allowing a colder snow cover to produce meltwater as it is entrained, as demonstrated by Steinkogler et al (2014).

It is significant that we were able to generate run-out distances in the 70-120% range in #934 Whiskey with very small release volumes. These long run-out distances are direct results of entrainment. Entrainment of snow -1°C or colder feeds dilation and stagnates the internal heat production by cooling the avalanche. The lack of initiated meltwater production appears to be the factor stopping avalanches at 70-80%.
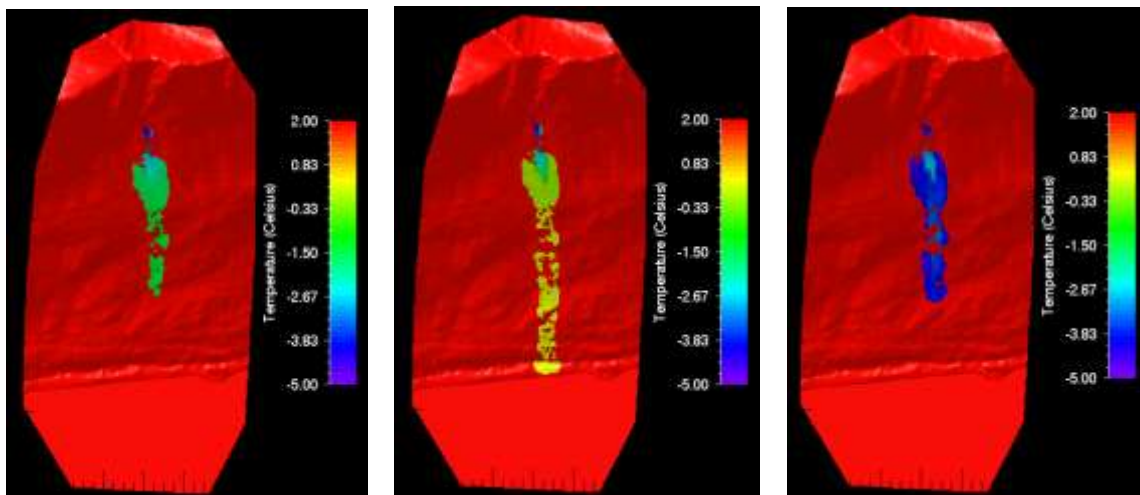

Fig. 11: (Left) Temperature of ED 0.25 m TE -5°C. Fig. 12: (Middle) Temperature of ED 0.25 TE 0°C. Fig. 13: (Right) Temperature of ED 0.5 m TE -5°C.

As soon as snow warmer than -1°C is entrained at an erosion depth of at least ~ 0.25 m, the added thermal heat dramatically increase the run-out distance to 120% and longer. During winter storms at Bird Hill the freezing level may reach up to ~ 800 m a s l or higher. Consequently, rapid warming of the snow surface is worth close attention for more accurate assessments of avalanche run-out distances. Hazardous snow cover properties can be correlated to weather data and monitored from weather stations. Next we will examine further how changes in the snow cover at a particular elevation may alter the flow regime.

The first investigations on the role of snow entrainment in avalanche motion considered only the mass balance of large (> 100 000 m^3) avalanches. Studies concentrated on the size of the release zone in relation to the amount of snow the avalanche could entrain. We have now refined these initial studies by introducing three new elements into the entrainment problem: (1) the role of snow temperature, (2) the question how entrained snow modifies the avalanche flow regime and (3) the influence of avalanche terrain. The modelling results suggest that all three problems are interrelated and allow no simple conclusion. Long avalanche run-out distances can be obtained under a variety of conditions. At present we can qualitatively duplicate the full range of avalanche activity at Bird Hill, but remain uncertain if our modelling assumptions and physics are correct. In the next project phase, we will reproduce historical and newly documented avalanche events at Bird Hill. The modelling helps constrain the parameters we gather in our field investigations. At present this might be the major advantage of modelling avalanches at a specific site.

ACKNOWLEDGEMENTS

REFERENCES

Alaska Department of Transportation & Public Facilities, 2013: *Avalanche data archive* [Available through Matt Murphy at Alaska Department of Transportation & Public Facilities, Girdwood, AK]

Bartelt, P., O. Buser, Y. Bühler, L. Dreier and M. Christen, M., 2014: Numerical simulation of snow avalanches: Modelling dilatative processes with cohesion in rapid granular shear flows. *Numerical Methods in Geotechnical Engineering* – Hicks, Brinkgreve & Rohe (Eds), Taylor & Francis Group, 327-332

Bartelt, P., Y. Bühler, O. Buser, M. Christen and L. Meier, 2012: Modeling mass-dependent flow regime transitions to predict the stopping and depositional behavior of snow avalanches. *Journal of Geophysical Research*, 117, 1-28.

Buser, O. and P. Bartelt, 2009: Production and decay of random kinetic energy in granular snow avalanches. *Journal of Glaciology*, 55, 189

Bartelt, P., O. Buser and K. Platzer, 2007: Frictional mechanisms at the tails of finite-sized mass movements. *Geophysical Research Letters*, 34, 1-6

Bühler, Y., M. Christen, J. Kowalski and P. Bartelt, 2011: Sensitivity of snow avalanche simulation to digital elevation model quality and resolution. *Annals of Glaciology*, 52, 58, 72-80.

Colbeck, S. C., 1975: Grain and bond growth in wet snow Snow mechanics: Proceedings of a symposium held at Grindelwald, 1974, *IAHS Publication*, 114, p 51-61

Christen, M., J. Kowalski and P. Bartelt, 2010: RAMMS: Numerical simulation of dense snow avalanches in three-dimensional terrain. *Cold Regions Science and Technology*, 63, 1-2, 1 – 14

Dent, J. D., K. J. Burrell, D. S. Schmidt, M. Y. Louge, E. Adams and T. G. Jazbutis, 1998: Density, velocity and friction measurements in a dry snow avalanche. *Annals of Glaciology*, 26, 247-252

Erismann, T. H., and G. Abele, 2001: *Dynamics of Rockslides and Rockfalls*, Springer Science & Business Media, 316

Gauer, P., D. Issler, D., K. Lied, K., K. Kristensen and F. Sandersen, 2008: On snow avalanche flow regimes: Inferences from observations and measurements, Proceedings of the *International Snow Science Workshop*, Whistler, Canada

Onesti, L. J., 1987: Slushflow release mechanism: A first approximation *Avalanche Formation, Movement and Effects*, no 162

Pudasaini, S. P. and K. Hutter, 2007: *Avalanche Dynamics. Dynamics of Rapid Flows of Dense Granular Avalanches*, Springer, 602

Steinkogler, W., B. Sovilla and M Lehning, 2014: Influence of snow cover properties on avalanche dynamics. *Cold Regions Science and Technology*, 97, 121-131

Vera Valero, C., T. Feistl, W. Steinkogler, O. Buser and P. Bartelt, 2012: Thermal Temperature in Avalanche Flow. Proceedings of *the International Snow Science Workshop*. Anchorage, AK. 32-37.

Vera, C. and P. Bartelt, 2013: Modelling Wet Snow Avalanche Flow with a Temperature Dependent Coulomb Friction Function. Proceedings of the *International Snow Science Workshop*. Grenoble, France. 691-696.